Proliferative arrest and rapid turnover of thymic epithelial cells expressing Aire

Daniel Gray, Jakub Abramson, Christophe Benoist, and Diane Mathis

Section on Immunology and Immunogenetics, Joslin Diabetes Center, Department of Medicine, Brigham and Women's Hospital, Harvard Medical School, Boston, MA 02215

Expression of autoimmune regulator (Aire) by thymic medullary epithelial cells (MECs) is critical for central tolerance of self. To explore the mechanism by which such a rare cell population imposes tolerance on the large repertoire of differentiating thymocytes, we examined the proliferation and turnover of Aire$^+$ and Aire$^-$ MEC subsets through flow cytometric analysis of 5-bromo-2′deoxyuridine (BrdU) incorporation. The Aire$^+$ MEC subset was almost entirely postmitotic and derived from cycling Aire$^-$ precursors. Experiments using reaggregate thymic organ cultures revealed the presence of such precursors among Aire$^-$ MECs expressing low levels of major histocompatibility complex class II and CD80. The kinetics of BrdU decay showed the Aire$^+$ population to have a high turnover. Aire did not have a direct impact on the division of MECs in vitro or in vivo but, rather, induced their apoptosis. We argue that these properties strongly favor a "terminal differentiation" model for Aire function in MECs, placing strict temporal limits on the operation of any individual Aire$^+$ MEC in central tolerance induction. We further speculate that the speedy apoptosis of Aire-expressing MECs may be a mechanism to promote cross-presentation of the array of peripheral-tissue antigens they produce.

CORRESPONDENCE
Christophe Benoist
OR
Diane Mathis:
cbdm@joslin.harvard.edu

To guard against autoimmunity, the thymus imposes self-tolerance on differentiating thymocytes. For conventional α/β T cells, this function is performed primarily by dendritic cells and thymic epithelial cells (TECs). It has emerged that TECs ectopically express a wide array of peripheral-tissue antigens (PTAs), a representation of self that substantially expands the scope of central tolerance (1). This promiscuous gene expression is compromised in humans and mice lacking the autoimmune regulator (AIRE; Aire in mice), leading to autoimmunity that targets a range of organs and tissues. Aire's tolerogenic function acts via medullary epithelial cells (MECs), because loss of the protein in these cells alone is necessary and sufficient to cause autoimmunity (2). How this rare cell population comes to express such a large and heterogeneous array of PTAs, how it manages to effectively purge the enormous repertoire of maturing thymocytes, and what implications this vast ectopic expression of proteins has for its own biology remain open questions.

Two models, both based on familiar paradigms in the field of developmental biology, have been proposed to explain Aire's function in MECs. The "terminal differentiation" model is rooted in the finding that a hierarchy of promiscuous gene expression exists among TEC subsets (3). It is postulated that increasingly promiscuous expression correlates with MEC differentiation and the CD80^{hi}, MHC II^{hi} subset of MECs (MEC^{hi}), which expresses Aire and the most PTA genes, representing the most mature cell type (1). Two predictions of this model are that, among TECs, individual MEC^{hi} express the most diverse array of PTAs, and that these cells are postmitotic products that ultimately perish (i.e., they are terminally differentiated; Fig. 1).

The competing "developmental" or "progressive restriction" model posits that Aire expression and promiscuous gene transcription are properties of immature precursor TECs (4). According to this scenario, Aire drives the differentiation of MECs into progressively restricted cell fates that recapitulate the transcriptional programs of different epithelial lineages. Therefore, it is predicted that the transcripts present in an individual mature MEC should reflect one such program. Furthermore, the Aire$^+$ MECs should be an immature, cycling cell type (Fig. 1).

One of the key distinguishing features of the two models is the differentiation state of Aire$^+$ MECs. The recent description of a precursor of Aire$^+$ MECs in the fetal thymus indicated that

The Journal of Experimental Medicine

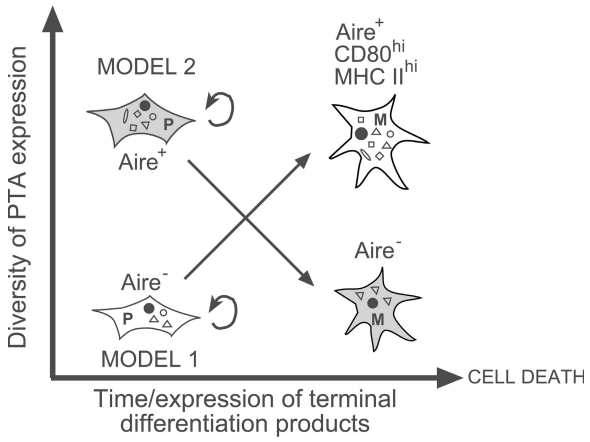

Figure 1. Distinguishing features of two models of TEC differentiation. A schematic diagram of two models of TEC differentiation from precursors (P) into mature MECs (M) in terms of the diversity of PTA expression versus time and differentiation. The terminal differentiation model (model 1) proposes that TEC precursors are Aire$^-$, cycling cells expressing few PTAs that give rise to mature, Aire$^+$, CD80^{hi}, MHC II^{hi} MECs that express the greatest diversity of PTAs. Conversely, the progressive restriction model (model 2) predicts that precursor TECs are Aire$^+$, cycling cells that express the greatest range of PTAs and differentiate down specific lineages into mature TECs expressing PTAs of terminally differentiated cells.

this subset is a downstream product in the MEC lineage (5); however, it remains to be determined how far downstream this is and whether the same sequence of differentiation holds for the steady-state adult thymus. In contrast, evidence of a high rate of cell division for the adult MEC^{hi} population (6, 7), the subset with the highest Aire levels, was interpreted to support the notion that these cells represent cycling precursors (8).

In this paper, we have exploited flow cytometric analysis of BrdU incorporation to provide a cell-by-cell view of the dynamics of the various MEC populations in adult mice. The data obtained support the terminal differentiation model and argue that Aire may not only drive expression of PTA but also promotes cellular changes to enhance their cross-presentation.

RESULTS AND DISCUSSION

Phenotypic characterization of Aire$^+$ MECs

The *Aire* gene is transcribed predominantly in the MEC^{hi} subset (3, 7), but it was not known how homogeneously these cells express the Aire protein. Therefore, we performed flow cytometric analysis of adult thymic stroma using an mAb specific for Aire (Fig. 2 A) (9). Intracellular staining of enriched TEC suspensions from *aire*$^{-/-}$ mice gave no signal but revealed a subset of Aire$^+$ cells composing 50–60% of the MEC^{hi} population in *aire*$^{+/+}$ mice (Fig. 2 B). A very low proportion of MEC^{lo} were Aire$^+$, whereas no staining above background was detected in cortical epithelial cell (CECs; Fig. 2 B). These values translated to an average of 8.4×10^4 ($\pm 2.5 \times 10^4$) Aire$^+$ MECs in the thymus of a 6-wk-old mouse.

Aire$^+$ MEC^{hi} were not distinguished from Aire$^-$ MEC^{hi} by expression of the MEC cell-surface markers, *Ulex europeaus* agglutinin 1 (UEA-1; Fig. 2 C) and CD80 (not depicted), nor by expression of a range of other markers previously associated with precursor cell types, including CD24, CD44, K5, K8, or Sca-1 (not depicted). However, both the Aire$^+$ and Aire$^-$ MEC^{hi} subsets expressed CD86 and programmed death 1 ligand (PD-L1) at variable levels (Fig. 2 C), indicating further heterogeneity among MEC^{hi} and the potential to provide distinct co-stimulation signals to thymocytes. Nonetheless, we found the phenotypes of Aire$^+$ and Aire$^-$ MEC^{hi} to be very similar overall.

Aire$^+$ MECs are postmitotic

The proliferative status of Aire$^+$ MECs is important for determining whether the terminal differentiation or progressive restriction model better describes MEC differentiation. A terminally differentiated population would be postmitotic, whereas, conversely, a precursor MEC population would rely on division for maintenance and phenotypic diversification. Previous studies showed that the adult MEC^{hi} subset was more proliferative than CECs and MEC^{lo}, according to assessments of DNA content (6), Ki67 expression (7), and BrdU labeling (7); however, the Aire$^+$ MEC^{hi} component was not specifically analyzed. On the other hand, relying on immunohistology, Hamazaki et al. found that adult Aire$^+$ MECs did not incorporate BrdU 4 h after injection (5), but this technique precluded quantitative analysis, and it was not clear whether this time point labeled sufficient MECs for detection. In this study, we optimized flow cytometric analysis of TECs for concurrent detection of BrdU and Aire to assess proliferation of Aire$^+$ and Aire$^-$ TEC subsets, and we also followed the flow of BrdU label with time to investigate their population dynamics.

First, to assess the relative levels of cell division among TEC subsets, we injected mice with a single dose of BrdU, waited 12h, stained enriched suspensions of thymic stromal cells with antibodies to TEC markers and BrdU, and analyzed them by flow cytomety. A substantial proportion of TECs had incorporated BrdU 12 h after injection (Fig. 3 A). In accordance with previous studies (6, 7), there was considerably lower incorporation by the MEC^{lo} compared with the MEC^{hi} population (average of 7.1 ± 2.9% vs. 15 ± 2.7%, respectively). Within the MEC^{hi} subset, the Aire$^-$ population had a surprisingly high level of BrdU incorporation, with 27% of the cells in this subset dividing during the pulse (Fig. 3 A). In contrast, minimal BrdU incorporation was detected in the Aire$^+$ MEC^{hi} subset, indicating that few, if any, Aire$^+$ cells were cycling (Fig. 3 A). Second, to follow the short-term fate of cells that divided during the BrdU pulse, we measured BrdU retention by TECs at various time points after injection. Within the whole TEC population, labeled cells diminished by one third within the first 3 d, then stabilized for the next 2 d (Fig. 3 B, far left). The pattern of decay was similar in the MEC^{lo} and Aire$^-$ MEC^{hi} subsets at magnitudes reflecting their initial BrdU incorporation (Fig. 3 B, left and right).

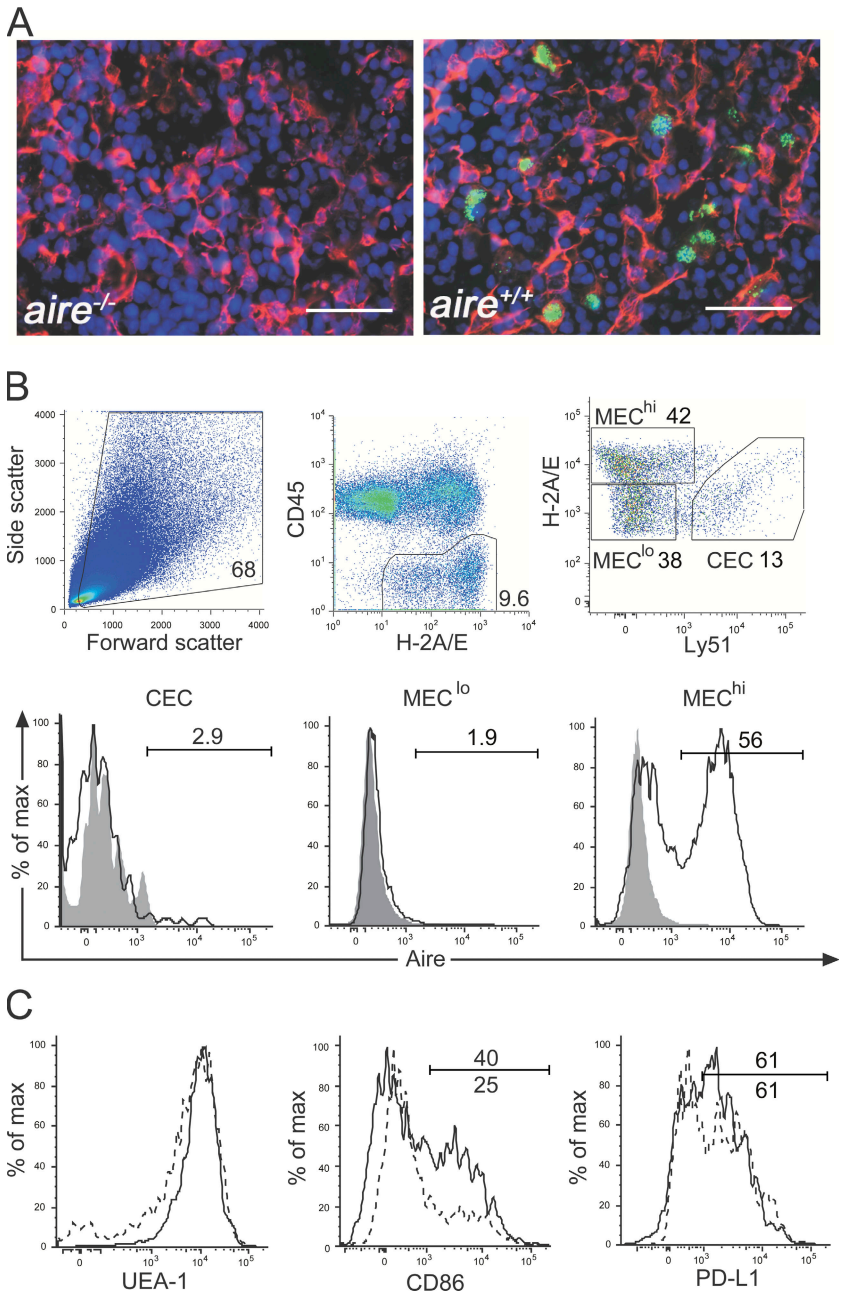

Figure 2. Phenotypic analysis of Aire$^+$ MECs. (A) Immunofluorescent staining of *Aire*$^{+/+}$ or *Aire*$^{-/-}$ thymus sections with anti-Aire (green), anti–cytokeratin-5 (K5; red), and DAPI (blue). Bars, 50 μm. (B, top) Dot plots show gating, from left to right, used to distinguish three major TEC subsets (CEC, MEC^{lo}, and MEC^{hi}) present in thymi from 6-wk-old mice. (bottom) Histograms of Aire expression in TEC subsets from *aire*$^{+/+}$ (continuous line) and *aire*$^{-/-}$ (shaded) mice. Numbers denote the proportion of cells in gated regions. (C) Expression of UEA-1, CD86, and PD-L1 in Aire$^+$ (continuous line) and Aire$^-$ (dashed line) MEC^{hi} are shown, with percentages of CD86$^+$ and PD-L1$^+$ MEC^{hi} in Aire$^+$ (top) and Aire$^-$ (bottom) subsets. Plots are representative of two to five experiments.

In contrast, the proportion of BrdU$^+$ cells in the Aire$^+$ MEC^{hi} population increased over the first 3 d after the pulse, then diminished (Fig. 3 B, far right). Given that Aire$^+$ MEC^{hi} were not cycling, the entry of BrdU into this compartment must be derived from cycling Aire$^-$ precursors.

To assess the turnover of these populations, we analyzed the kinetics of BrdU incorporation over a 2-wk period of constant access to label. The proportion of cycling cells at the outset of incorporation was assessed 2 h after BrdU injection. Again, the Aire$^-$ MEC^{hi} population incorporated the most BrdU and Aire$^+$ MEC^{hi} only background levels (Fig. 3 C, right and far right), confirming the data in Fig. 3 A, which used a longer pulse. Interestingly, almost all Aire$^-$ MEC^{hi} were BrdU$^+$ by 5.5 d (Fig. 3 C, right), indicating that this

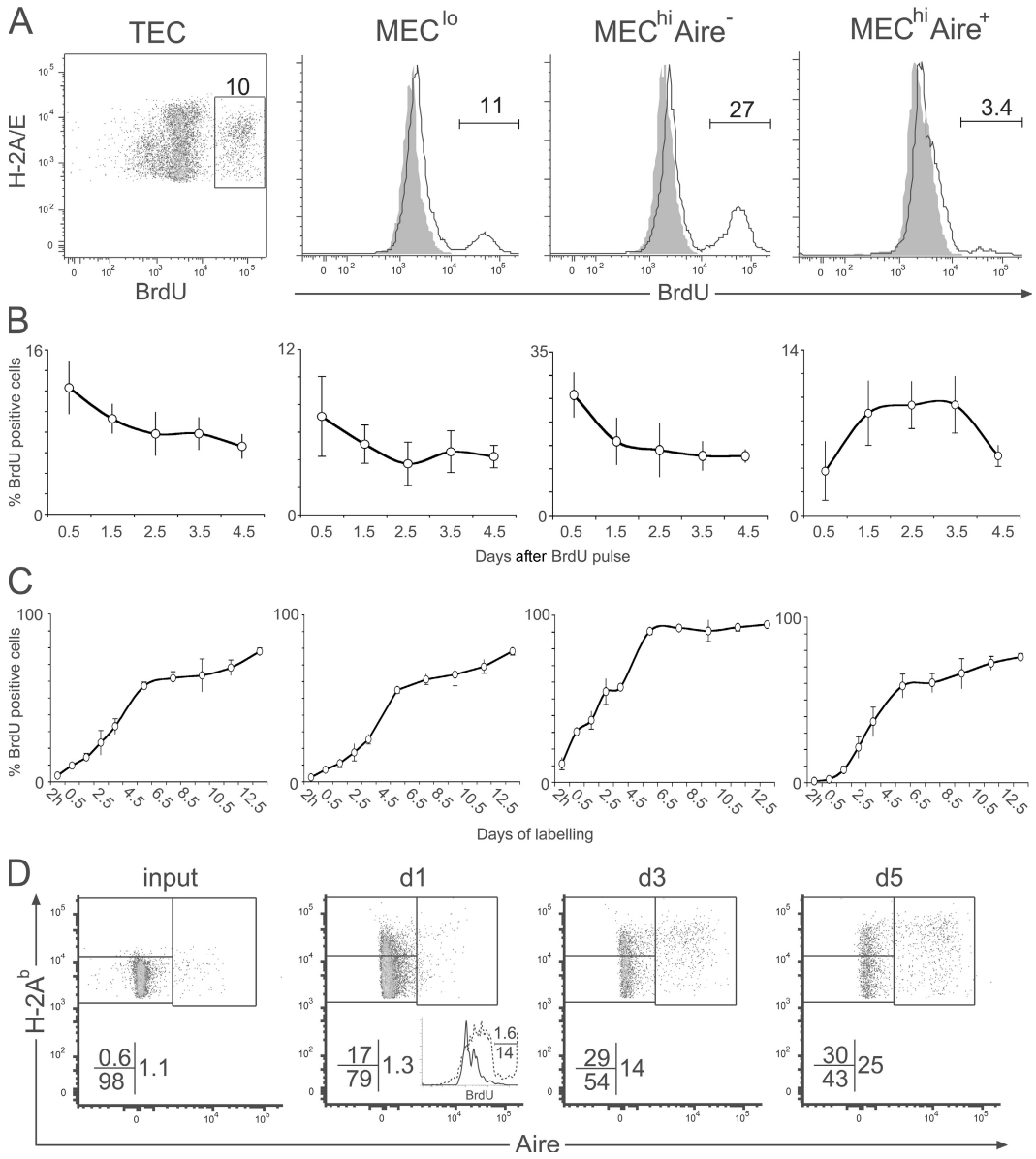

Figure 3. Aire$^+$ MECs are postmitotic and turn over rapidly. (A) Mice were pulsed with BrdU, and TECs were analyzed 12 h later for BrdU incorporation. Uninjected controls (shaded) and percentages of BrdU$^+$ cells from injected mice (continuous line) are shown. (B) BrdU decay kinetics in TEC populations after a single pulse (values represent the mean ± SD). (C) BrdU incorporation kinetics in TEC populations during a 2-wk exposure (values represent the mean ± SD). Data are representative of three to five experiments, with each using three to four mice per time point. (D) Adult B6 MEC^{lo} were reaggregated with E15.5 B6.H-2^{g7} stroma with SP thymocytes, and Aire expression on H-2^{b+} MECs was analyzed during culture. Regions and corresponding values show the proportion of Aire$^-$ MEC^{lo}, Aire$^-$ MEC^{hi}, and Aire$^+$ MECs. (inset) BrdU staining on Aire$^+$ (continuous line) and Aire$^-$ (dotted line) H-2^{b+} MECs. Data are representative of three experiments.

subpopulation is composed entirely of rapidly dividing cells with a prodigious replacement rate of 20% per day. In contrast, the TEC, MEC^{lo}, and Aire$^+$ MEC^{hi} subsets showed bimodal incorporation curves, with saturation of a rapidly dividing component (~60% of each) within 6 d, followed by a reduced rate of incorporation by a component with a lower level of proliferation (Fig. 3 C, far left, left, and right). This result indicates that mixtures of cells with both high and low turnover rates maintain these subsets.

A lag period of 36 h before BrdU$^+$ cells accumulated in the Aire$^+$ MEC^{hi} population (Fig. 3 C, far right) reflected the precursor/product relationship observed in the decay kinetics and represents the minimum amount of time such a precursor takes to up-regulate Aire after cell division. Taking this delay into account, we estimate that an average of 13% (±2.1%) of this subset is replaced each day.

The slow turnover of MEC^{lo} and their expression of the putative TEC precursor marker, MTS-24 (10), are reminiscent

of immature epithelial cells in other tissues (11). To determine whether adult MEC^{lo} were indeed precursors of Aire$^+$ MECs, MEC^{lo} were purified and reaggregated with MHC-mismatched embryonic stroma and adult CD4/8 single-positive (SP) thymocytes. After 5 d of culture, a substantial proportion and number of MEC^{lo} had up-regulated MHC II and Aire (Fig. 3 D). Aire$^+$ MECs did not incorporate BrdU in vitro (Fig. 3 D), indicating that there was no expansion of trace Aire$^+$ MEC^{lo} and, therefore, that Aire$^-$ MEC^{lo} were differentiating into the Aire$^+$ cells observed. A proportion of these Aire$^+$ cells were MHC II^{lo}, perhaps reflecting slower kinetics of differentiation in vitro compared with in vivo and/or differential provision of the signals driving Aire and MHC II molecule up-regulation. Collectively, the observations that Aire$^+$ MEC^{hi} are postmitotic and are derived from cycling, Aire$^-$ MEC^{lo} precursors establish that Aire expression is a late event in MEC differentiation.

Rapid turnover of Aire$^+$ MECs

To investigate the fate of Aire$^+$ MEC^{hi}, we analyzed their longevity in BrdU decay experiments. Mice were exposed to BrdU for 2 wk to achieve maximal incorporation (80–100%); label was then withdrawn and retention was measured at various times thereafter. During the chase period, BrdU$^+$ TECs diminished in both label intensity and proportion labeled, suggesting further division by cycling cells and loss of cells by apoptosis or some other means (Fig. 4).

Continued cycling, manifest as reduced BrdU intensity, was evident for the Aire$^-$ MEC^{lo} and MEC^{hi} subsets (unpublished data). The presence of a relatively large proportion of MEC^{lo} with high levels of BrdU 4 wk after label withdrawal (unpublished data) indicates a low level of turnover and is in accord with low levels of division.

The label in the noncycling Aire$^+$ MEC^{hi} subset showed a rapid decline, with 90% of labeled cells gone 2 wk after withdrawal of BrdU (Fig. 4). The rate of loss during the first 2 wk (6.5% per day) is likely to be an underestimate (compared with the 13% per day observed in the incorporation study) because of the continued entry of labeled precursors during this time. Nevertheless, these data indicate very rapid turnover of this population relative to the Aire$^-$ MEC^{hi} and MEC^{lo} subpopulations.

The finding that Aire$^+$ MEC^{hi} are postmitotic and have a high turnover rate raises the question of whether Aire itself causes proliferative arrest and/or apoptosis of MEC. This notion was supported by the finding that *aire*$^{-/-}$ mice have an increased proportion and number of MEC^{hi} (Fig. 5 A, dot plots) (2) at the expense of the MEC^{lo} subset (Fig. 5 A, right). To determine whether this increase was caused by greater proliferation of MEC^{hi} in the absence of Aire, we injected BrdU into *aire*$^{+/+}$ and *aire*$^{-/-}$ mice and analyzed incorporation by MEC^{hi} 12 h later. Surprisingly, the proportion of BrdU$^+$ MEC^{hi} in *aire*$^{-/-}$ mice was significantly lower than in *aire*$^{+/+}$ controls, suggesting that the higher numbers of MEC^{hi} in *aire*$^{-/-}$ mice are not derived from increased proliferation but stem from expansion of postmitotic MEC^{hi} (i.e., analogous to Aire$^+$ MEC^{hi}; Fig. 5 B). Reduced Aire levels in *aire*$^{+/-}$ mice (9) did not impinge on the MEC^{hi} proportion, numbers, or BrdU incorporation (unpublished data). Therefore, Aire does not directly inhibit MEC^{hi} proliferation; rather, it modulates the overall number of the postmitotic population in some other way, perhaps by inducing apoptosis.

Studies of apoptosis in TECs ex vivo were not feasible because of the induction of high levels of Annexin V labeling and caspase activation by the thymus digestion procedure (unpublished data). Staining of thymus sections with the activated caspase marker VAD-FMK demonstrated in situ apoptosis of thymocytes but did not label Aire$^+$ or Aire$^-$ K5$^+$ TECs. This presumably reflects the fact that thymic macrophages and dendritic cells promptly phagocytose dying cells, as they do the vast majority of thymocytes that perish daily but escape detection by apoptosis assays (12). Therefore, we used the MEC cell line 1C6 to investigate a potential link between Aire expression and apoptosis.

To assess whether Aire overexpression could directly inhibit MEC division, we transfected 1C6 cells with vectors encoding either GFP or an Aire-GFP fusion protein and analyzed proliferation by BrdU incorporation. Comparable transfection efficiencies were observed in the two cultures (~30% GFP$^+$). Correct folding, localization, and activity of the fusion protein was confirmed by fluorescence microscopy, Western blotting, and gene array analysis of transcription by cells transfected with Aire-GFP, with up-regulation of many PTAs (unpublished data). The proportion of GFP$^+$ cells

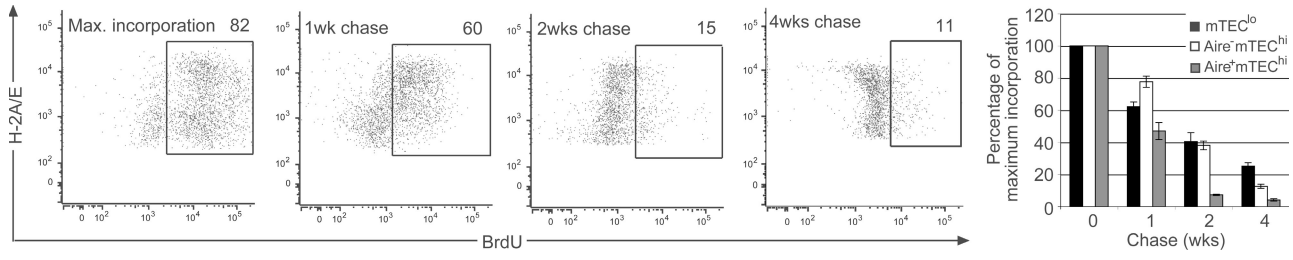

Figure 4. Rapid loss of Aire$^+$ MEC^{hi}. After a 2-wk BrdU incorporation period, label retention was assayed 1, 2, and 4 wk after withdrawal in whole TECs (dot plots). Gates were set according to uninjected controls for each experiment. Numbers denote the proportion of cells in gated regions. The bar graph plots the mean (±SD) proportion of maximum incorporation found for MEC^{lo}, Aire$^-$ MEC^{hi}, and Aire$^+$ MEC^{hi} from three mice per time point.

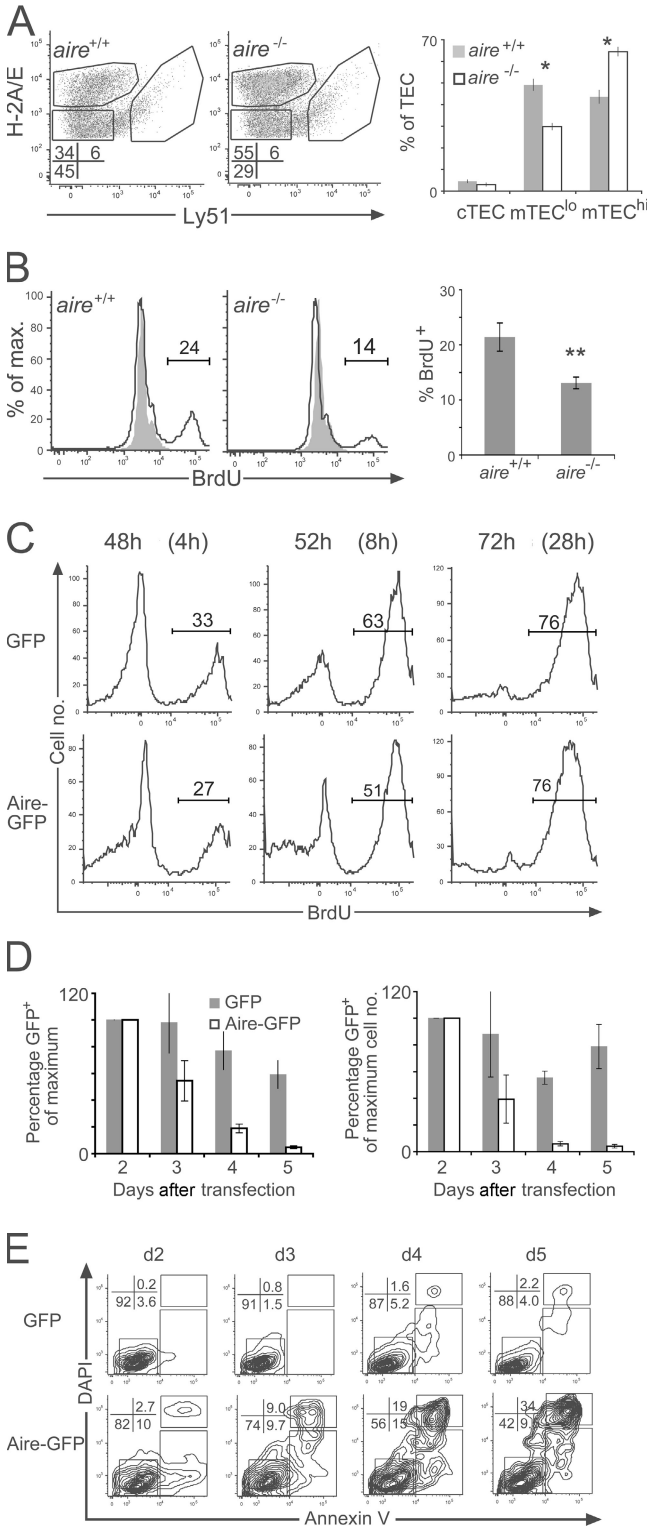

Figure 5. The Aire protein does not directly impinge on proliferation. (A) Dot plots gated on TECs from *aire*$^{+/+}$ or *aire*$^{-/-}$ mice with regions distinguishing CECs, MEC^{lo}, and MEC^{hi}. Bar graph shows mean (±SD) TEC subset proportions for *aire*$^{+/+}$ and *aire*$^{-/-}$ mice ($n = 4$). *, $P < 0.005$. (B) BrdU incorporation by MEC^{hi} from *aire*$^{+/+}$ or *aire*$^{-/-}$ mice was analyzed 12 h after pulse (continuous line), compared with uninjected controls (shaded). (right) Bar graph of mean (±SD) percentage of BrdU$^+$ MEC^{hi} in *aire*$^{+/+}$ or *aire*$^{-/-}$ mice ($n = 5$). **, $P < 0.05$. (C) The 1C6 MEC line was transfected with GFP or Aire-GFP expression constructs, and BrdU was added to the cultures 44 h later. The percentage of GFP$^+$ cells incorporating BrdU is shown for plots representative of two experiments at various time points after transfection (time with BrdU is shown in parentheses). (D) Bar graphs of mean (±SD) percent GFP$^+$ of maximum proportion or cell number (at 2 d) in GFP- or Aire-GFP–transfected cultures over time ($n = 3$). (E) GFP$^+$ cells were analyzed for Annexin V binding and uptake of DAPI at various time points after transfection. Plots are representative of three experiments, with regions distinguishing viable (Annexin$^-$/DAPI$^-$), early apoptotic (Annexin$^+$/DAPI$^-$), and late apoptotic (Annexin$^+$/DAPI$^+$) MECs.

incorporating BrdU was not substantially different between 2 and 3 d after transfection, indicating that Aire-GFP did not affect proliferation (Fig. 5 C). However, both the proportion and number of Aire-GFP$^+$ MECs were decreased compared with GFP$^+$ MECs from 3 d after transfection, declining until no Aire-GFP$^+$ cells were detected after 5 d, whereas about one half of the GFP$^+$ MECs remained (Fig. 5 D). Importantly, the specific loss of Aire-GFP–expressing MECs was caused by increased apoptosis at all time points (Fig. 5 E). Similar results were obtained with an Aire-GFP construct containing an internal ribosomal entry site before the GFP sequence, indicating that apoptosis was caused specifically by Aire (unpublished data). These data establish that overexpression of Aire does not directly inhibit MEC division but rather induces apoptosis. This finding offers a likely explanation for the paucity of MEC lines that express Aire.

Conclusions

This study revealed several important aspects of TEC differentiation and population dynamics. A surprisingly high rate of turnover for the entire TEC population of 10% per day (±0.7%) was in accordance with previous estimates (7) and was driven by proliferation, predominantly within the Aire$^-$ MEC^{hi} subset. The rapid cycling of all cells in this subset strongly suggests that it constitutes an MEC transit-amplifying population that may regulate parameters such as overall numbers of MECs and the tempo of their differentiation. The finding that certain TECs are highly proliferative also raises questions regarding the long-held assumption that TECs are relatively radioresistant because of low mitotic activity: does radiation in fact cause loss of TEC subsets and subsequent defects in thymocyte differentiation and tolerance?

Direct analysis of BrdU incorporation by Aire$^+$ MECs at the single-cell level revealed that, in the adult, these cells are postmitotic and derive from a cycling precursor. While this paper was under review, Rossi et al. (13) showed maturation of E15 CD80$^-$ to CD80$^+$ MECs but also that CD80 was not a surrogate marker for Aire expression. Transcription of *Aire* in the ex vivo CD80$^-$ MEC subset left open the question of the precise identity of Aire$^+$ MEC precursors in the fetal thymus. High levels of CD80 and MHC II were better correlates for Aire expression in adult MECs, and reaggregate thymus organ culture of purified MEC^{lo} gave rise to Aire$^+$ MEC^{hi}, without

expansion of low-level (~1%) Aire$^+$ MEC^{lo}. The low efficiency of MEC^{lo} transition to Aire$^+$ MEC suggests that only a minor subpopulation of MEC^{lo} exhibits this potential. The influence of apoptosis on the emerging Aire$^+$ population does need to be taken into account, however, as does the possibility that not all MEC^{lo} are exposed to the necessary inductive signals in this system. Whether the differentiation of Aire$^-$ MEC^{lo} to Aire$^+$ MEC^{hi} occurs via an Aire$^-$ MEC^{hi} intermediate awaits the means to purify this latter population. Furthermore, the dependency of this adult differentiation program upon signals important for fetal Aire$^+$ MECs (i.e., the requirement of RANK signals) (13) remains to be determined.

The Aire$^+$ MEC^{hi} population has a high turnover, with loss of cells most likely through apoptosis, based on the in vivo kinetics of decay and in vitro overexpression studies. The possibility that some in vivo loss of BrdU$^+$ Aire$^+$ MEC^{hi} occurs by cells down-regulating Aire and joining another subset cannot be ruled out. Nevertheless, the findings of this study are consistent with the terminal differentiation model and not the progressive restriction model of TEC differentiation.

The induction of apoptosis by Aire further supports the finality of its activity in MEC differentiation. Interestingly, the highest levels of apoptosis were seen 4 d after transfection, suggesting that Aire may initiate a sequence of events that culminates in MEC death. This scenario raises the question of whether apoptosis occurs via direct induction of an apoptotic program or indirectly through up-regulation of PTA that overload the protein synthesis machinery to such an extent as to provoke death through ER stress. Regardless, the delay in apoptosis should allow sufficient time for the promiscuous expression of genes by MECs, followed by cell death to deliver a battery of PTAs to dendritic cells for cross-presentation and induction of central tolerance to peripheral self (14). Thus, to affect central tolerance, Aire may not only induce transcription of PTA but also promote cellular changes that ensure their efficient presentation.

MATERIALS AND METHODS

Mice. Aire-deficient mice were derived and genotyped as previously described (2) and were analyzed on the C57BL/6 (B6) × 129 genetic background. Mice were housed at the Center for Animal Resources and Comparative Medicine at the Harvard Medical School, and the Institutional Animal Care and Use Committee approved procedures. BrdU labeling experiments were initially performed with 6–8-wk-old NOD × B6 mice, then with B6 mice for final replicates. B6.H-2^{g7} mice (15) were time mated, and the day of vaginal plug detection was designated E0.5.

BrdU administration. BrdU was administered as previously described (16). In brief, mice were injected intraperitoneally with 1 mg BrdU (Sigma-Aldrich) in PBS to provide a labeling pulse. Continuous labeling was maintained by incorporation of 0.8 mg/ml BrdU in sterile drinking water with artificial sweetener. 8-wk-old mice were used for this experiment because thymic stromal cell numbers remain essentially at steady state during the labeling period (7).

Fluorescent reagents and flow cytometry. The following antibodies, purchased from BD Biosciences unless otherwise stated, were used: rabbit anti–mouse K5 (Covance), rat anti-Aire (rat IgG2c, clone 5H12; a gift from H. Scott, Walter and Eliza Hall Institute of Medical Research, Melbourne, Australia), anti–I-A/E–Pacific blue and –allophycocyanin (APC; clone M5/114.15.2; BioLegend), biotinylated anti-Ly51 (clone 6C3), anti-CD45–PerCP-Cy5.5 (clone 30-F11), anti-BrdU–Alexa Fluor 488 (clone 3D4; Caltag), UEA-1–FITC (Vector Laboratories), anti-CD86–PE (clone GL1), anti–PD-L1–PE (clone M1H5), anti–rat IgG2c-PE and -FITC (clone 2C-8F1; Southern Biotechnology Associates, Inc.), Cy3-conjugated donkey anti–rabbit IgG (Jackson ImmunoResearch Laboratories), Annexin-V–PE, and streptavidin-APC.Cy7 and -APC. Suspensions of thymic stromal cells were prepared as previously described (17). All digests were counted and analyzed for TEC enumeration, and totals were compared using the Student's *t* test. Intracellular Aire staining was performed using fixation/permeabilization buffers (eBioscience) according to the manufacturer's instructions. For BrdU experiments, the second of two enzymatic digestions of individual thymi was used for analysis. Stromal cells were fixed/permeabilized using BD Bioscience buffers, followed by paraformaldehyde/Tween 20, and were treated with DNase (50 Kunitz units) before staining with anti-BrdU. Data were acquired on a flow cytometer (LSR II; BD Biosciences) and analyzed using FloJo software (TreeStar, Inc.).

Reaggregate thymus organ cultures. MEC^{lo} and SP thymocytes from B6 mice were sorted to >97% purity on a cytometer (MoFlo; DakoCytomation), as previously described (7). MEC^{lo} and SP thymocytes were reaggregated with suspensions of fresh E15.5 embryonic stroma from B6.H-2^{g7} mice, as previously described (13), at ratios of 1:1:8. Reaggregates were dispersed in dispase/DNase for flow cytometric analysis. For analysis of proliferation, 10 μM BrdU was added 5 h before termination of the culture.

Immunohistology. 8-μm air-dried cryosections of thymus were stained with primary antibodies for 30 min and then subjected to three 5-min washes in PBS. Secondary antibodies were incubated for 30 min, followed by washes. Sections were then incubated in DAPI (Invitrogen) for 5 min, washed, and mounted with coverslips in aqueous mounting medium (Biomeda). Images were acquired with a confocal microscope (Axiovert 200M; Carl Zeiss MicroImaging, Inc.) using a xenon-arc lamp in a wavelength switcher (Lambda DG-4; Sutter Instrument Co.) and processed with Slidebook imaging software (Intelligent Imaging Inc.).

Cell lines and transfection. The 1C6 cell line, originally derived from mouse MECs (18), was a gift of M. Kasai (National Institute of Infectious Diseases, Tokyo, Japan). Cells were seeded onto 12-well plates (at 10–20% confluence) and transfected with Effectene (QIAGEN) and 300 ng of either *aire* cloned into pEGFP-c1 expression vectors (Aire-GFP) or 300 ng of pEGFP-c1 (GFP) 16 h later. Transfected 1C6 cells were harvested at a various time points, and the relative intensity of GFP was analyzed by flow cytometry. Apoptosis was measured with Annexin V and DAPI staining, and GFP$^+$ MECs were analyzed by flow cytometry.

We thank Dr. Hamish Scott, Dr. Michiyuki Kasai, and Mr. Andrew Koh for reagents.

This work was supported by grant RO1 DK60027 from the National Institutes of Health and Young Chair funds to D. Mathis and C. Benoist, and by Joslin's National Institutes of Diabetes and Digestive and Kidney Diseases–funded Diabetes and Endocrinology Research Center core facilities. D. Gray received support from an Australian National Health and Medical Research C.J. Martin Overseas Biomedical Fellowship, and J. Abramson received support from the Juvenile Diabetes Research Foundation.

The authors have no conflicting financial interests.

Submitted: 19 April 2007
Accepted: 7 September 2007

REFERENCES

1. Kyewski, B., and L. Klein. 2006. A central role for central tolerance. *Annu. Rev. Immunol.* 24:571–606.
2. Anderson, M.S., E.S. Venanzi, L. Klein, Z. Chen, S.P. Berzins, S.J. Turley, H. von Boehmer, R. Bronson, A. Dierich, C. Benoist, and D. Mathis. 2002. Projection of an immunological self shadow within the thymus by the aire protein. *Science.* 298:1395–1401.

3. Derbinski, J., J. Gabler, B. Brors, S. Tierling, S. Jonnakuty, M. Hergenhahn, L. Peltonen, J. Walter, and B. Kyewski. 2005. Promiscuous gene expression in thymic epithelial cells is regulated at multiple levels. *J. Exp. Med.* 202:33–45.
4. Gillard, G.O., and A.G. Farr. 2005. Contrasting models of promiscuous gene expression by thymic epithelium. *J. Exp. Med.* 202:15–19.
5. Hamazaki, Y., H. Fujita, T. Kobayashi, Y. Choi, H.S. Scott, M. Matsumoto, and N. Minato. 2007. Medullary thymic epithelial cells expressing Aire represent a unique lineage derived from cells expressing claudin. *Nat. Immunol.* 8:304–311.
6. Yang, S.J., S. Ahn, C.S. Park, K.L. Holmes, J. Westrup, C.H. Chang, and M.G. Kim. 2006. The quantitative assessment of MHC II on thymic epithelium: implications in cortical thymocyte development. *Int. Immunol.* 18:729–739.
7. Gray, D.H., N. Seach, T. Ueno, M.K. Milton, A. Liston, A.M. Lew, C.C. Goodnow, and R.L. Boyd. 2006. Developmental kinetics, turnover, and stimulatory capacity of thymic epithelial cells. *Blood.* 108:3777–3785.
8. Gillard, G.O., J. Dooley, M. Erickson, L. Peltonen, and A.G. Farr. 2007. Aire-dependent alterations in medullary thymic epithelium indicate a role for Aire in thymic epithelial differentiation. *J. Immunol.* 178:3007–3015.
9. Liston, A., D.H. Gray, S. Lesage, A.L. Fletcher, J. Wilson, K.E. Webster, H.S. Scott, R.L. Boyd, L. Peltonen, and C.C. Goodnow. 2004. Gene dosage–limiting role of Aire in thymic expression, clonal deletion, and organ-specific autoimmunity. *J. Exp. Med.* 200:1015–1026.
10. Gill, J., M. Malin, G.A. Hollander, and R. Boyd. 2002. Generation of a complete thymic microenvironment by MTS24(+) thymic epithelial cells. *Nat. Immunol.* 3:635–642.
11. Nijhof, J.G., K.M. Braun, A. Giangreco, C. van Pelt, H. Kawamoto, R.L. Boyd, R. Willemze, L.H. Mullenders, F.M. Watt, F.R. de Gruijl, and W. van Ewijk. 2006. The cell-surface marker MTS24 identifies a novel population of follicular keratinocytes with characteristics of progenitor cells. *Development.* 133:3027–3037.
12. Surh, C.D., and J. Sprent. 1994. T-cell apoptosis detected in situ during positive and negative selection in the thymus. *Nature.* 372: 100–103.
13. Rossi, S.W., M.Y. Kim, A. Leibbrandt, S.M. Parnell, W.E. Jenkinson, S.H. Glanville, F.M. McConnell, H.S. Scott, J.M. Penninger, E.J. Jenkinson, et al. 2007. RANK signals from $CD4^{+}3-$ inducer cells regulate development of Aire-expressing epithelial cells in the thymic medulla. *J. Exp. Med.* 204:1267–1272.
14. Gallegos, A.M., and M.J. Bevan. 2004. Central tolerance to tissue-specific antigens mediated by direct and indirect antigen presentation. *J. Exp. Med.* 200:1039–1049.
15. Luhder, F., J. Katz, C. Benoist, and D. Mathis. 1998. MHC class II molecules can protect from diabetes by positively selecting T cells with additional specificities. *J. Exp. Med.* 187:379–387.
16. Tough, D.F., and J. Sprent. 1994. Turnover of naive- and memory-phenotype T cells. *J. Exp. Med.* 179:1127–1135.
17. Gray, D.H., A.P. Chidgey, and R.L. Boyd. 2002. Analysis of thymic stromal cell populations using flow cytometry. *J. Immunol. Methods.* 260:15–28.
18. Mizuochi, T., M. Kasai, T. Kokuho, T. Kakiuchi, and K. Hirokawa. 1992. Medullary but not cortical thymic epithelial cells present soluble antigens to helper T cells. *J. Exp. Med.* 175:1601–1605.